Available online at www.sciencedirect.com
ScienceDirect
Mathematics and Computers in Simulation xxx (xxxx) xxx
MATHEMATICS AND COMPUTERS IN SIMULATION
www.elsevier.com/locate/matcom

Original articles

Photovoltaic single-diode model parametrization. An application to the calculus of the Euclidean distance to an $I-V$ curve

F. Javier Toledo[a,*], Vicente Galiano[b], Jose M. Blanes[c], Victoria Herranz[a], Efstratios Batzelis[d]

[a] *Center of Operations Research, Miguel Hernández University of Elche, Spain*
[b] *Computers Engineering Department, Miguel Hernández University of Elche, Spain*
[c] *Industrial Electronics Group, Miguel Hernández University of Elche, Spain*
[d] *Electronics and Computer Science, University of Southampton, United Kingdom*

Received 23 August 2022; received in revised form 14 December 2022; accepted 3 January 2023
Available online xxxx

Abstract

In this paper we provide a new parametrization of the characteristic curve (I-V curve) associated to the photovoltaic (PV) single-diode model (SDM), which is the most common model in the literature to analyze the behavior of a PV panel. The SDM relates the voltage with the current, through a transcendental equation with five parameters to be determined. There are many methodologies to extract the SDM parameters and some of them are based on obtaining the best fit of the SDM model on a voltage–current dataset through the ordinary least squares method. However, the fact that errors affect not only the current but also the voltage indicates that the maximum likelihood estimation (MLE) of the parameters is obtained by the total least squares method, also called orthogonal distance regression (ODR). The main difficulty in performing ODR lies in obtaining the Euclidean distance from a point to the SDM I-V curve which is in general a hard mathematical problem; in our particular case it is noticeably more difficult due to the implicit nature of the SDM equation and the fact that solution candidates might not be unique. This paper proposes a new parametrization that allows reduction of the calculus of the Euclidean distance from any point to the I-V curve to solving a single-variable equation. An in-depth mathematical analysis determines the number of possible candidates where the Euclidean distance can be attained. Moreover, a full casuistry alongside a geometrical study based on the curvature of the I-V curve and the Maximum Curvature Point, permits identification and classification of all these candidates. This enables for the first time a complete algorithm to compute the Euclidean distance from a point to an I-V curve at any condition and, thus, to perform a reliable ODR to obtain the MLE of the SDM parameters. Using the obtained theoretical background, it is demonstrated that two existing methodologies to compute the Euclidean distance fail in some cases, whereas the proposed algorithm is execution-proof and runs faster.

Keywords: Photovoltaics; Single-diode model; Parametrization; Euclidean distance; Orthogonal distance regression; Total least squares

* Correspondence to: Center of Operations Research, Miguel Hernández University, 03202 Elche, Spain.
E-mail addresses: javier.toledo@umh.es (F.J. Toledo), vgaliano@umh.es (V. Galiano), jmblanes@umh.es (J.M. Blanes), mavi.herranz@umh.es (V. Herranz), e.batzelis@soton.ac.uk (E. Batzelis).

https://doi.org/10.1016/j.matcom.2023.01.005

Please cite this article as: F.J. Toledo, V. Galiano, J.M. Blanes et al., Photovoltaic single-diode model parametrization. An application to the calculus of the Euclidean distance to an $I-V$ curve, Mathematics and Computers in Simulation (2023), https://doi.org/10.1016/j.matcom.2023.01.005.

1. Introduction

The calculation of the Euclidean distance from a point to a curve in the plane $\mathbb{R}^2$, also referred to as orthogonal distance or perpendicular distance, is a mathematical problem that consists of finding the minimum distance from the point to the curve. This distance, defined through the Euclidean norm or the 2-norm in $\mathbb{R}^2$, finds applications in numerous engineering problems, especially in the broad field of parameters identification. In the particular case that the curve is a straight line, the problem is quite simple and the solution is given by a very well-known closed-form formula (see, for example, [41]). For any other type of curve, the distance problem becomes much more complicated (see, for example, [24] for the distance to a conic), especially when the curve is given implicitly or the solution candidates mare multiple (not unique). This paper deals with such an application on photovoltaic (PV) modeling, in which we want to calculate the Euclidean distance from a voltage–current point to the characteristic curve (I-V curve) generated with the single-diode model (SDM) equation which implicitly relates the voltage and the current.

The SDM, also known as five-parameter model, is surely the most widely used approach to characterize the behavior of a PV module (e.g. Google Scholar yields more than 95,000 results to a search of keywords *photovoltaic single diode model*). Obtaining the SDM parameters has been an active research topic for more than 50 years and is still at the forefront of research today. A short review that follows aims to provide a glimpse of the state of the art on this area. The following studies use experimental data to extract the parameters. In particular, [8] obtains the maximum likelihood estimates (MLE) of the parameters by using the Euclidean distance; [16,30,44] have obtained in recent years very promising results in the parameters extraction by minimization based on the current distance; and [28] analyzes in depth various fitting approaches, including a novel method that combines current and voltage distances. As an alternative approach, [43] provides an analytical and quasi-explicit method for parameters extraction without the use of fitting techniques. Other papers use the manufacturers' datasheet for the parameters extraction; for example, [31,45] demonstrate that only with the three Remarkable Points (short-circuit, open-circuit and maximum power points), there are infinite I–V curves satisfying these conditions. Other papers analyze the parameters behavior as functions of the environmental conditions (see, for example, [9,20,26]), or other factors such as degradation (see, for example, [6,27,39]). There are many methodologies to obtain the SDM parameters from a set of voltage–current points obtained from experimental measurements, some of which are based on approximations and simplifications of the model. Examples are assuming infinite shunt resistance, R_{sh}, [10,46]; treating the ideality factor, n, as a constant [47]; neglecting the series resistance, R_s [21]; as well as approximations of the equations derived from the model being forced to satisfy the Remarkable Points conditions, that is, the short circuit point, $(0, I_{sc})$, the open circuit point, $(V_{oc}, 0)$ and maximum power point, (V_{mpp}, I_{mpp}), satisfy the SDM equation and the slope at the maximum power point, I'_{mpp}, satisfy the relation $I'_{mpp} = -I_{mpp}/V_{mpp}$ (see, for example, [7,19,38]).

One of the most efficient methodologies for the calculation of the parameters is the so-called "Reduced form method" [29,30]. This is based on finding closed relations between the parameters by using the remarkable points conditions in order to reduce the number of parameters to be determined, then these independent parameters are obtained by means of curve fitting with the rest of available points. [16] is another paper that uses the idea of reducing the dimension of the parameter search space in combination with a generalized Benders-like decomposition, it obtains similar results to [30]. Nevertheless, the methodology that today obtains the best results over two case studies (originally used in [22] and nowadays usually used in the literature to compare parameter extraction methods) and on the one million curves dataset of National Renewable Energy Laboratory (NREL), is the so-called "Two-step linear least-squares method" [44]. This is based on the "Oblique Asymptote method", inspired by the geometric properties of the SDM [42], in conjunction with the least-squares method. It is also possible to obtain good parameters directly by performing a curve fitting method starting from certain parameters acquired by simple strategies. Other methods adopt sophisticated optimization techniques such as metaheuristic algorithms (for example, genetic [5,37], generalized reduced gradient [33], particle swarm [1], pattern search [2], simulated annealing [23], artificial bee colony [36], adaptive differential evolution [17] , harmony searchbased [3], or salp swarm [35]), but some of them need to know a priori bounds on the parameters that can be obtained, for example, from the remarkable points using the formulae provided in [45], see also [31].

In almost all the optimization methodologies, the objective function consists of minimizing an error metric based on the current, usually the Root Mean Square Error (RMSE). However, it has been shown quite a few times in the literature that this approach may skew the results when the samples feature noise in both voltage and current. A very recent paper [8] has demonstrated that the maximum likelihood parameters estimation (MLE) is obtained only when the metric is based on the Euclidean distance from a voltage–current point to the I–V curve instead of the current

distance. This means that the calculation of the Euclidean distance becomes a key tool in photovoltaic modeling. A few studies prior to the one just mentioned have used to date the Euclidean distance metric for the calculation of the model parameters. [15] applies orthogonal distance regression (ODR) to find the model parameters that minimize the sum of squared orthogonal distances from each data point to the model surface in the core of their model calibration algorithm. [15] uses the well-known ODRPACK software ([11,12]) based on an algorithm to perform ODR [13,14]. This algorithm has an inner loop that attempts to find the Euclidean distance from each sample (x_i, y_i) to the model curve as follows: consider a finite collection of points on a neighborhood $[a, b]$ of x_i and, then compute the corresponding points of the model curve which, moreover, satisfy the orthogonality condition (OC) (i.e. the tangent line to the model curve at a model point is orthogonal to the line crossing this point and (x_i, y_i), that is checked with an independent routine). This inner loop has some computational limitations, namely, it is not guaranteed that the window $[a, b]$ provides a point of the model curve where the OC is satisfied, and it is not certain that the point is the global minimum, as we show later that this is a problem with multiple solutions. Moreover, the accuracy and speed of the algorithm will depend on the number of points taken in $[a, b]$. These limitations can occur, for example, when (x_i, y_i) is not sufficiently close to the model curve or the interval $[a, b]$ is not sufficiently large. Other methods to compute the Euclidean distance from a point to an I–V curve suffer again in providing a solution without checking if it really is the global minimum, which occurs particularly when multiple candidates are available. These are the main challenges in two benchmark methods we evaluate in this paper: (i) the system of two nonlinear equations formed by the SDM equation and the necessary optimality condition, and (ii) a recent method which reduces the previous system in a one-variable equation based on the so-called diode voltage [8].

This paper treats this problem comprehensively by theoretically studying the Euclidean distance calculation on SDM and introducing an algorithm that guarantees correct and reliable solution. This method is based on a new parametrization of the SDM (Section 2), which allows to reduce the calculation of the Euclidean distance to compute the roots of a one-variable function. This function has been deeply studied to locate all its possible roots and infer whether they are possible candidates to provide the Euclidean distance (Section 3). Furthermore, this study explores for the first time relevant geometrical concepts, such as the curvature of a I–V curve and the corresponding calculus of the maximum curvature point of a I–V curve alongside the identification of its evolute (Section 3.3 and Appendix A). The resulting foolproof ED algorithm (Section 4) is then applied to orthogonal distance regression for high accuracy and fast execution time. The proposed parametrization is useful for other applications as well related to photovoltaic modeling. Finally, these findings are supported by experimental tests (Section 5) that demonstrate the reliability of the ED Algorithm (Appendix A) as compared to the existing state of the art.

2. A photovoltaic single-diode model parametrization

This section introduces a parametrization of the I–V curve associated to the SDM and explains the meaning and other implications of the parameters defined.

2.1. New parametrization

The single-diode model (SDM) equation associated to a solar panel with n_s cells in series is given by

$$I = I_{ph} - I_{sat}\left(\exp\left(\frac{V + I\ R_s}{n_s n V_T}\right) - 1\right) - \frac{V + I\ R_s}{R_{sh}} \tag{1}$$

where I is the panel current, V is the panel voltage, I_{ph} is the panel photocurrent, I_{sat} is the panel diode saturation current, R_s is the panel series resistance and, R_{sh} is the panel shunt resistance. The value n is the ideality factor, and $V_T = \frac{k}{q}T$ is the so-called thermal voltage, where T is the temperature, k is the Boltzmann's constant and, q is the electron charge.

Eq. (1) can be rewritten (see, for example, [42], and [44])as

$$I = A + B - EV - BC^V D^I \tag{2}$$

where

$$A = \frac{I_{ph} Rsh}{R_{sh} + R_s},\ B = \frac{I_{sat} Rsh}{R_{sh} + R_s},\ E = \frac{1}{R_{sh} + R_s},\ C = \exp\left(\frac{1}{n_s n V_t}\right),\ D = \exp\left(\frac{R_s}{n_s n V_t}\right). \tag{3}$$

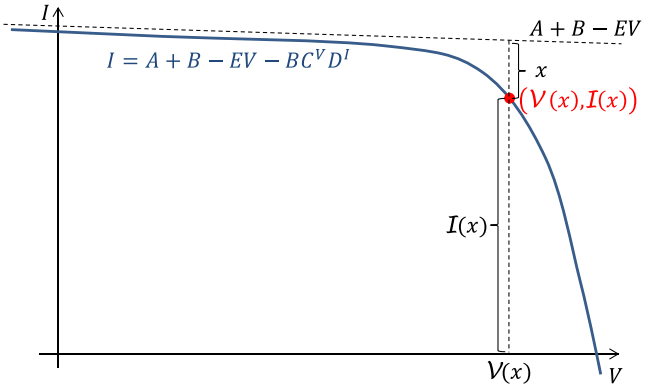

Fig. 1. Geometrical parameter meaning in the parametrization (7).

If we define $x = BC^V D^I > 0$, taking logarithms one has

$$\ln x = \ln B + V \ln C + I \ln D \tag{4}$$

In addition, substituting $x = BC^V D^I$ in Eq. (2) yields

$$I = A + B - EV - x \tag{5}$$

Now, combining (4) and (5) one obtains

$$\ln x = \ln B + V \ln C + (A + B - EV - x) \ln D$$

from where V can be isolated exclusively in terms of x as

$$V = \frac{1}{\ln C - E \ln D} (\ln x - (A + B - x) \ln D - \ln B) \tag{6}$$

Finally, if V in (5) is replaced by its expression in (6), I becomes as follows exclusively in terms of x

$$I = A + B - E \left(\frac{1}{\ln C - E \ln D} (\ln x - (A + B - x) \ln D - \ln B) \right) - x$$

Therefore, we have established that any point of the I–V curve (2) is of the form $(\mathcal{V}(x), \mathcal{I}(x))$ for certain positive x, where

$$\begin{cases} \mathcal{V}(x) = \frac{1}{\ln C - E \ln D} (\ln x - (A + B - x) \ln D - \ln B) \\ \mathcal{I}(x) = A + B - E\mathcal{V}(x) - x \end{cases} \tag{7}$$

In other words, $(\mathcal{V}(x), \mathcal{I}(x))$ is a parametrization of the I–V curve.

It is worth noting that all the previous formulation and the subsequent development can be expressed in terms of the original parameters I_{ph}, I_{sat}, n, R_{sh}, and R_s but, as we will see in Section 3, the expressions and results are simpler and easier to interpret using parameters A, B, C, D, and E.

These explicit expressions of V and I as functions of the auxiliary variable x have many applications and will be a key tool here in the precise and fast calculation of the Euclidean distance from a point to an I–V curve.

2.2. On the parameter x of the new parametrization

Geometrically speaking, the parameter x in the I–V curve parametrization (7) given by

$$x = BC^V D^I = A + B - EV - I \in]0, +\infty[$$

is the vertical distance of the I–V point $(\mathcal{V}(x), \mathcal{I}(x))$ to the asymptote oblique $A + B - EV$ of (1) and (2) (see Fig. 1).

2.2.1. The parameter x as a function of V or I

I and V can be expressed in terms of the Lambert W function, W_0 (see [4]), and the expressions using the parameters A, B, C, D, and E are shown in (8) and (9).

$$I = A + B - EV - \frac{1}{\ln D} W_0\left(BC^V D^{A+B-EV} \ln D\right) \tag{8}$$

$$V = \frac{1}{E}(A + B - I) - \frac{1}{\ln C} W_0\left(\frac{B}{E} D^I C^{\frac{1}{E}(A+B-I)} \ln C\right) \tag{9}$$

Comparing the second equation in (7) with (8) and (9) one deduces the following expressions for the parameter x in terms of V and I via the Lambert W function.

$$x(V) = \frac{1}{\ln D} W_0\left(BC^V D^{A+B-EV} \ln D\right)$$

$$x(I) = \frac{E}{\ln C} W_0\left(\frac{B}{E} D^I C^{\frac{1}{E}(A+B-I)} \ln C\right)$$

2.2.2. The parameter x as a function of the derivative function I′ and vice versa: the slope of the I–V curve at any point

Eq. (2) defines I as an infinitely differentiable function of the variable V (see [42]). Differentiating implicitly with respect to V in (2) one obtains

$$I' = -E - BC^V D^I \left(\ln C + I' \ln D\right)$$

and by exploring that $BC^V D^I = x$ one has

$$I' = -E - x\left(\ln C + I' \ln D\right)$$

from where

$$x\left(I'\right) = -\frac{I' + E}{\ln C + I' \ln D} \quad \text{and} \quad I'(x) = -\frac{E + x \ln C}{1 + x \ln D} \tag{10}$$

In [42], it was established $-\frac{\ln C}{\ln D} < I' < -E$, so $\ln C + I' \ln D > 0$ and $I' + E < 0$.

Please observe that the second expression in (10) gives directly the slope of the I–V curve at any point (V, I) through

$$I'(V, I) = -\frac{E + BC^V D^I \ln C}{1 + BC^V D^I \ln D} = -\frac{E + (A + B - EV - I) \ln C}{1 + (A + B - EV - I) \ln D} \tag{11}$$

This above relationship (11) has been already given in [42].

In the following, the new parametrization given in (7) along with the properties derived from it, is applied to obtain the Euclidean distance from a point to an I–V curve defined by the SDM equation. The novelty of this parametrization paves the way also to other applications in photovoltaic modeling.

3. The Euclidean distance from a point to an I–V curve: an in-depth analysis

3.1. Problem reduction

The problem of finding the point(s) of the I–V curve, corresponding to the SDM (2), closest with respect to the Euclidean distance to a given point (V_0, I_0) can be modeled as the following mathematical optimization problem

$$\begin{array}{ll} \text{Minimize} & (V - V_0)^2 + (I - I_0)^2 \\ \text{subject to} & I = A + B - EV - BC^V D^I \end{array} \tag{12}$$

Using the parametrization (7), the optimization problem (12) is reduced to minimize the single-variable function

$$d(x) = (\mathcal{V}(x) - V_0)^2 + (\mathcal{I}(x) - I_0)^2 \tag{13}$$

where $x \in]0, +\infty[$.

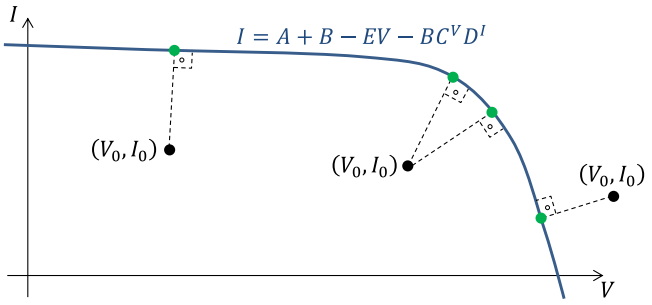

Fig. 2. Graphical representation of closest points of an I–V curve from a point (V_0, I_0).

The example of Fig. 2 shows three different points (in black), their corresponding closest points on the I–V curve (in green) and the Euclidean distance (dashed lines). It is worth noting that there may be multiple solutions to that problem, as Fig. 2 illustrates.

3.1.1. Properties of function d

In order to analyze the possible extremes of d given in (13), let us study the properties of function d and its first and second differentiated functions. These properties are given below.

- d is infinitely differentiable on its domain $]0, +\infty[$.
- $\lim_{x\to 0^+} d(x) = +\infty$ and $\lim_{x\to+\infty} d(x) = +\infty$.
- The derivative function of d can be written as (see the details in Appendix C)

$$d'(x) = \frac{2}{\delta^2 x} f(x)$$

where

$$f(x) = (\alpha + \beta x)\ln x + \gamma x^2 + \eta x + \rho \tag{14}$$

with

$$\begin{aligned}
\alpha &= 1 + E^2 \\
\beta &= \ln D + E \ln C \\
\gamma &= (\ln C)^2 + (\ln D)^2 \\
\delta &= \ln C - E \ln D \\
\eta &= \beta(1 - \ln B) - \gamma(A + B) + \delta(I_0 \ln C - V_0 \ln D) \\
\rho &= -(\alpha \ln B + \beta(A + B) + \delta(V_0 - E I_0))
\end{aligned} \tag{15}$$

For SDM parameters with physical meaning, α, β and γ are positive (see (3)), but also δ is positive because $E < \ln C / \ln D$ (see again (3)). Please observe that α, β, γ and δ do not depend on (V_0, I_0), whereas η and ρ are functions of (V_0, I_0).

Remark: Obviously, the critical points of d ($d'(x) = 0$) are the roots of the function f ($f(x) = 0$). Moreover, d' and f have the same sign.

3.1.2. Properties of function f

Let us study the properties of function f given in (16) and next, its implications on d' and d.

- f is infinitely differentiable on its domain $]0, +\infty[$.
- $\lim_{x\to 0^+} f(x) = -\infty$ and $\lim_{x\to+\infty} f(x) = +\infty$
- From the previous properties, f has at least one root on $]0, +\infty[$
- $f'(x) = \frac{1}{x}(\alpha + \beta x) + \beta \ln x + 2\gamma x + \eta = \frac{1}{x}\left(\beta x \ln x + 2\gamma x^2 + (\beta + \eta)x + \alpha\right)$
- $\lim_{x\to 0^+} f'(x) = +\infty$ and $\lim_{x\to+\infty} f'(x) = +\infty$

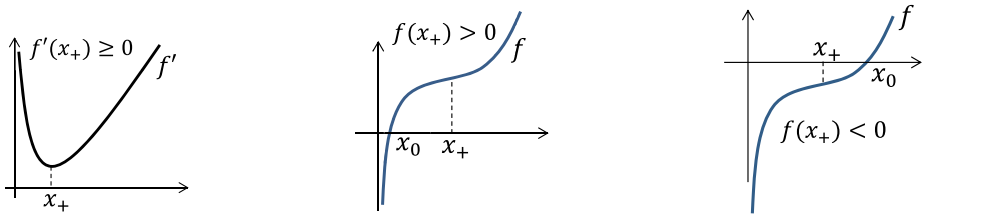

(a) Graph of f'. Case $f'(x_+) \geq 0$ (b) Graph of f. Subcase $f(x_+) \geq 0$ (c) Graph of f. Subcase $f(x_+) < 0$

Fig. 3. Shapes of f' and f when $f'(x_+) \geq 0$.

- $f''(x) = \frac{-\alpha}{x^2} + \frac{\beta}{x} + 2\gamma$
- $f''(x) = 0 \Leftrightarrow x = -\frac{1}{4\gamma}\left(\beta + \sqrt{\beta^2 + 8\alpha\gamma}\right) < 0$ (out of the domain of f) or $x = \frac{1}{4\gamma}\left(\sqrt{\beta^2 + 8\alpha\gamma} - \beta\right) > 0$.

Due to its relevance in the results of this work, let us denote

$$x_+ = \frac{1}{4\gamma}\left(\sqrt{\beta^2 + 8\alpha\gamma} - \beta\right) \tag{16}$$

3.2. Critical points of the distance function d

From the above properties of f, one has that its derivative function f' is decreasing on $]0, x_+[$ and increasing on $]x_+, +\infty[$ and, so, f' attains on $]0, +\infty[$ a unique relative (indeed global) minimum at x_+. Based on this, the following casuistry analyzes all the possible cases to find and classify the critical points of d and, as a consequence, it allows to obtain in any case the global minimum of d.

1. If $f'(x_+) \geq 0$, then $f' \geq 0$ on $]0, +\infty[$ and, consequently, f is increasing on $]0, +\infty[$, then f and d' have a unique root x_0 on $]0, +\infty[$, which is the unique critical point of d (in fact the global minimum of d). See illustrative examples in Fig. 3.
2. If $f'(x_+) < 0$, f' has two roots, x_1 and x_2, with $0 < x_1 < x_2$, such that $f' > 0$ on $]0, x_1[\cup]x_2, +\infty[$ and $f' < 0$ on $]x_1, x_2[$, then function f has a relative maximum at x_1 and a relative minimum at x_2.
   Two subcases are distinguished:

   (a) If $f(x_1) \leq 0$ or $f(x_2) \geq 0$, then f and d' have a unique root x_0 on $]0, +\infty[$, which is the unique critical point of d, (in fact the global minimum of d). More concretely:

   - If $f(x_1) < 0$ or $f(x_2) > 0$, then f and d' have a unique root x_0 on $]0, +\infty[$ (see Fig. 4).
   - If $f(x_1) = 0$ or $f(x_2) = 0$, f and d' have a pair of different roots (see Fig. 5).
     - If $f(x_1) = 0$ and x_0 is the other root, then $x_1 < x_0$ and d attains a unique relative (in fact global) minimum at x_0 and an inflection point at x_1.
     - If $f(x_2) = 0$ and x_0 is the other root, then $x_2 > x_0$ and d attains a unique relative (in fact global) minimum at x_0 and an inflection point at x_2.

   (b) If $f(x_1) > 0$ and $f(x_2) < 0$, f has three roots x_{01}, x_{02} and x_{03}, with $x_{01} < x_{02} < x_{03}$, where d attains, respectively, minimum, maximum and minimum relatives, then, the global minimum of d cannot be attained at x_{02}. Just comparing $d(x_{01})$ and $d(x_{03})$ one knows which is the global minimum of d (see Fig. 6).

Remark: From the previous casuistry it is concluded that there are at most three candidates to attain the Euclidean distance from a point to the I–V curve and, in fact they can be perfectly analytically classified. The main reason why existing methods may fail to find the Euclidean distance is because they do not analyze the number of possible candidates nor do they classify the candidates obtained. In contrast, this paper shows that leveraging on the previous analysis, a closed algorithm can be designed to obtain the solution(s) corresponding to the global minimum without any failures. The next subsection explains how this is achieved in a computationally efficient manner.

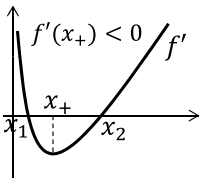

(a) Graph of f'. Case $f'(x_+) < 0$

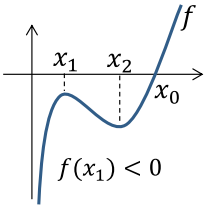

(b) Graph of f. Subcase $f(x_1) < 0$

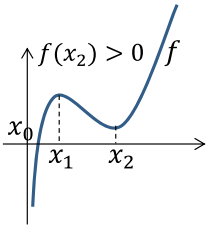

(c) Graph of f. Subcase $f(x_2) > 0$

Fig. 4. Shapes of f' and f when $f'(x_+) < 0$ and $f(x_1) < 0$ or $f(x_2) > 0$.

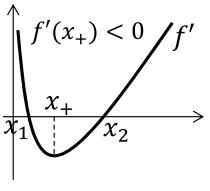

(a) Graph of f'. Case $f'(x_+) < 0$

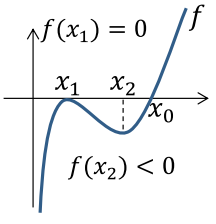

(b) Graph of f. Subcase $f(x_1) = 0$.

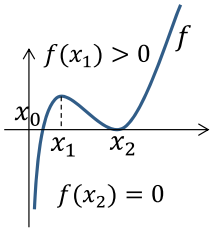

(c) Graph of f. Subcase $f(x_2) = 0$

Fig. 5. Shapes of f' and f when $f'(x_+) < 0$ and $f(x_1) = 0$ or $f(x_2) = 0$.

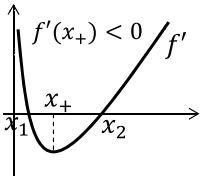

(a) Graph of f'. Case $f'(x_+) < 0$

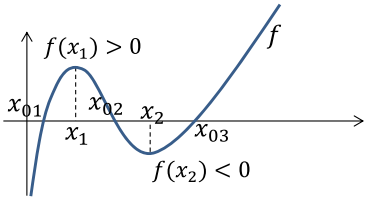

(b) Graph of f. Subcase $f(x_1) > 0$ and $f(x_2) < 0$

Fig. 6. Shapes of f' and f when $f'(x_+) < 0$ with $f(x_1) > 0$ and $f(x_2) < 0$.

3.3. A geometrical analysis of the critical points of d through the curvature of the I–V curve.

Previous subsection has proven that function f may have 1, 2 or 3 roots depending on the location of the samples (V_0, I_0) and that the candidate to the Euclidean distance is not always unique. However, it should be noted that for samples very close to the curve, f will exhibit usually just 1 root as explained later. Nevertheless, in many applications there are instances that some samples are far away from the curve, thus giving rise to multiple solutions, which is the reason why many algorithms fail. For example, in parameter extraction applications, a search algorithm may initialize and go through parameter values that correspond to curves which are distant to the samples.

In this subsection, we establish some interesting relationships between certain geometrical features of the I–V curve and the functions f and f'. These relationships along with the information provided in the previous subsection allows for a resourceful casuistry that reaches quickly and flawlessly the roots of f and therefore the Euclidean distance.

First of all, please observe that due to the strict concavity of the I–V curve (see [42]), for the points (V_0, I_0) above the I–V curve the function d has a unique critical point where its global minimum is attained.

Now, let us interpret the geometrical meaning of $f'(x_+) = 0$. Remember that, as seen in Section 3.2, the sign of $f'(x_+)$ is crucial to locate the roots of f.

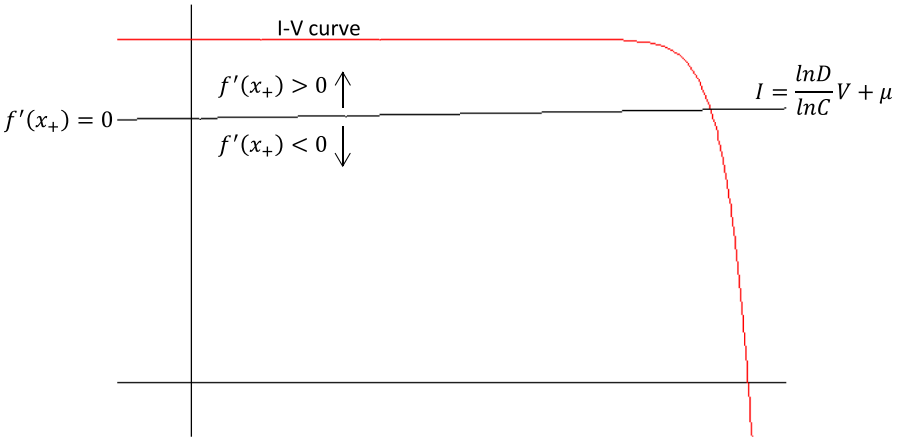

Fig. 7. Graphical representation of an I–V curve and its corresponding line $f'(x_+) = 0$.

Since $f''(x_+) = 0$, which is equivalent to $2\gamma x_+^2 = \alpha - \beta x_+$, the following equivalence can be derived from the expression of $f'(x_+)$

$$f'(x_+) = 0 \Leftrightarrow I_0 = \frac{\ln D}{\ln C} V_0 + \mu$$

where $\mu = \frac{1}{\delta \ln C}\left(\gamma (A+B) - \beta \ln\left(\frac{e\ x_+}{B}\right) - \frac{2\alpha}{x_+}\right)$ does not depend on the point (V_0, I_0) (see in Fig. 7 the geometric representation). Now, one has that $f'(x_+) > 0$ if, and only if, $I_0 > \frac{\ln D}{\ln C} V_0 + \mu$, and, as a consequence, $f'(x_+) < 0$ if, and only if, $I_0 < \frac{\ln D}{\ln C} V_0 + \mu$. In other words, if the point (V_0, I_0) is on the line $I = \frac{\ln D}{\ln C} V + \mu$ or above, then $f'(x_+) \geq 0$ and d has a unique critical point where it attains its global minimum. On the other hand, if the point (V_0, I_0) is below this line, then $f'(x_+) < 0$ and the second level of casuistry of Section 3.2 must be done to find the global minimum of d.

Next, let us interpret the geometrical meaning of $f(x_1) = 0$ and $f(x_2) = 0$ in the case $f'(x_+) < 0$.

3.3.1. Maximum curvature of an I–V curve: the maximum curvature point.

As we have already explained the beginning of this subsection, points "close enough" to the I–V curve satisfy that f has a unique root, i.e. d has a unique critical point where the global minimum distance is attained. As we show below, this is not a coincidence but a consequence of the proximity of the experimental points to the I–V curve alongside the curvature of the curve (see [40]).

In general, the *radius of curvature* of a curve at one of its points P_0 is the radius of the circular arc which best approximates the curve at this point. Formally, the *radius of curvature*, R, is the reciprocal of the *curvature*, k, let us define below. The circular arc is a portion of a circumference, *osculating circle*, of radius R, *curvature radius*, centered at a certain point O, *center of curvature*, and, therefore, this radius is the minimum distance from O to the curve. Moreover, the distance is attained, at least, at P_0, and thus, any other point P_1, on the segment connecting O and P_0, attains its minimum distance to the curve uniquely at P_0 (see [40]).

Let us provide the exact computation of the maximum curvature of an I–V curve.

The curvature of the function I is given by the formula (see [18] for a historical overview of the definition of curvature)

$$k = \frac{|I''|}{\left(1 + (I')^2\right)^{3/2}} = \frac{-I''}{\left(1 + (I')^2\right)^{3/2}}$$

where the second equality is a consequence of $I'' < 0$ (see for instance [42]).

One has the following expression of I'' in terms of I'

$$I'' = \frac{\left(\ln C + I' \ln D\right)^2}{\ln C - E \ln D}\left(I' + E\right)$$

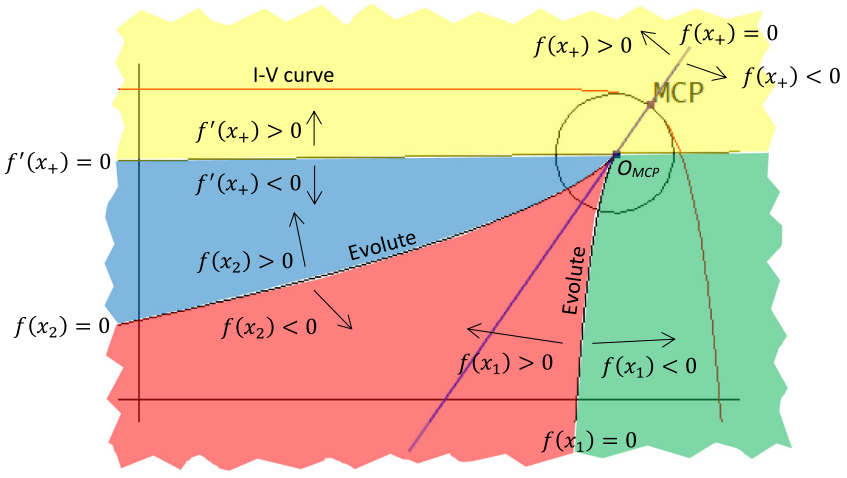

Fig. 8. Geometrical interpretation of the casuistry in the different regions of an I–V curve. Yellow, blue, green ($\mathcal{E}$) and O_{MCP}: f has 1 root; Evolute ($ext(\mathcal{E})$) (except O_{MCP}): f has 2 roots; Red ($int(\mathcal{E})$): f has 3 roots.

So, using the expression of I' in terms of x given in (10) one can express the curvature k in terms of x as (see details in Appendix C.2)

$$k(x) = \frac{\delta^2 x}{\left(\alpha + 2\beta x + \gamma x^2\right)^{3/2}}$$

where $\alpha, \beta, \gamma, \delta$ where given in (15).

Observe that the critical points of k (those where $k' = 0$) are exactly the same points where $f'' = 0$ (see details in Appendix C.3, see also Proposition 1.3 in [25], and [32]), recall $x = -\frac{1}{4\gamma}\left(\sqrt{\beta^2 + 8\alpha\gamma} + \beta\right) < 0$ (which is not a possible value) and $x = x_+ = \frac{1}{4\gamma}\left(\sqrt{\beta^2 + 8\alpha\gamma} - \beta\right) > 0$. Moreover, at $x = x_+$ function k attains a relative maximum which is in fact its global maximum on $]0, +\infty[$. So, the maximum curvature of the I–V curve is

$$k_{\max} = k(x_+) = \frac{\delta^2 x_+}{\left(\alpha + 2\beta x_+ + \gamma x_+^2\right)^{3/2}}$$

and it is attained at the "Maximum Curvature Point", $MCP = (V_{MCP}, I_{MCP})$, which is obtained from (7) for $x = x_+$.

The radius of curvature of the I–V curve at the MCP is $R_{\max} = 1/k_{\max}$ and the corresponding center of curvature is denoted by O_{MCP} (see Figs. 8 and 9).

One has that the line crossing the points MCP and O_{MCP} is exactly $f(x_+) = 0$, and the center of curvature of the MCP is the intersection point of the lines $f(x_+) = 0$ and $f'(x_+) = 0$ (see Fig. 8).

Fig. 8 shows that the place of all the centers of curvature of the I–V curve, called the *evolute of the curve*, provides a partition of the plane into three subsets: $\mathcal{E}$, $int(\mathcal{E})$, and $ext(\mathcal{E})$, given by:

1. $\mathcal{E}$: the evolute itself formed by two branches $f(x_1) = 0$ and $f(x_2) = 0$. The points in $\mathcal{E}$ necessarily satisfy $f'(x_+) \leq 0$.
2. $int(\mathcal{E})$: an open set between the two branches of the evolute and with the point O_{MCP} as a cusp, that is, the points satisfying $f'(x_+) < 0$ with $f(x_1) > 0$ and $f(x_2) < 0$ (red region in Fig. 8).
3. $ext(\mathcal{E}) = (\mathcal{E} \cup int(\mathcal{E}))^c$: the complementary set of $\mathcal{E} \cup int(\mathcal{E})$, that is, the points satisfying $f'(x_+) < 0$ with $f(x_1) < 0$ or $f(x_2) > 0$, or the points satisfying $f'(x_+) > 0$ (yellow, blue and green regions in Fig. 8).

Recall from the analytical casuistry that:

- If $(V_0, I_0) \in ext(\mathcal{E}) \cup O_{MCP}$, function f has a unique root where function d attains its global minimum.
- If $(V_0, I_0) \in \mathcal{E} \setminus O_{MCP}$, function f has two roots but function d has a unique global minimum in one of them.

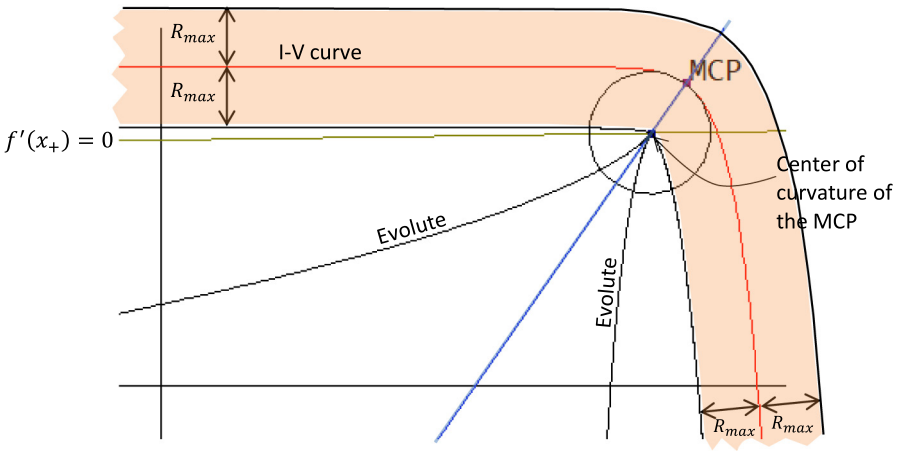

Fig. 9. Graphical representation of an I–V curve and its corresponding strip Λ.

- If $(V_0, I_0) \in int\,(\mathcal{E})$, function f has three roots and function d can attain its global minimum at one or at most at two of them.

Taking into account all the previous information, any point (V_0, I_0) with a distance to the I–V curve less than $R_{\max} = 1/k_{\max}$ falls into the set $ext\,(\mathcal{E})$. The set of these points is the strip colored in orange in Fig. 9.

So, coming back to our first comment in this subsection, an example of a real situation where the points are close enough to the I–V curve can be given when one has a set of I–V points measured with a certain noise level that is small enough for the noisy points to satisfy the conditions for f to have a unique root corresponding to the unique minimum of d. But even in this special case, some algorithms like N-R method may fail to converge to that solution if the seed used is not in the basin of attraction of the solution.

4. Proposed strategy to compute the Euclidean distance

In this section, we are employing all the theoretical information obtained in the previous subsections to design an algorithm that computes in any possible case the Euclidean distance from a point (V_0, I_0) to the I–V curve. We minimize the casuistry that turns around the value x_+ given in (16). In addition, in each possible position of the point (V_0, I_0), we provide a seed that ensures not only the convergence of the N-R method applied to f, but also that it is close to the solution to achieve a fast convergence. As can be seen in Fig. 10, the selection of the seeds for the N-R method applied to f, depends on the sign of $f\,(x_+)$; specifically, to ensure convergence of the method, if $f\,(x_+) > 0$ the seed x_s must be selected to the left of x_+ satisfying $f\,(x_s) < 0$ and, if $f\,(x_+) < 0$ the seed must be selected to the right of x_+ satisfying $f\,(x_s) > 0$ (see Appendix B.1 on how to obtain the concrete seeds proposed in the ED algorithm of Appendix A).

This selection of seeds guarantees moreover that:

- If f has 1 or 2 roots, that is, if (V_0, I_0) is inside the yellow, blue or green regions or on the black curve of the evolute in Fig. 8, the N-R method converges to the solution corresponding to the Euclidean distance.
- If f has 3 roots, that is, if (V_0, I_0) is inside the red region in Fig. 8, the N-R method achieves the two relative minima of d and, then, just a simple comparison will provide the one corresponding to the Euclidean distance.

Algorithm 1 designed to obtain the Euclidean distance, whose flowchart is shown in Fig. 11 and pseudocode can be found at Appendix A, has the following main steps:

1. *Initialization phase*: Compute the root x_{aux} of f obtained with a seed selected as explained before in terms of the sign of $f\,(x_+)$.
2. *Identification phase*: Check the position of the point (V_0, I_0) to distinguish the number of possible roots of f.

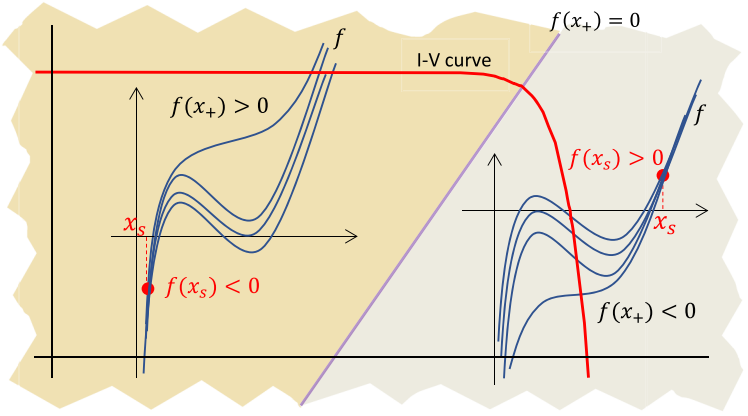

Fig. 10. Graphical representation of seeds selection in different parts of the I–V curve using the geometrical meaning of the casuistry.

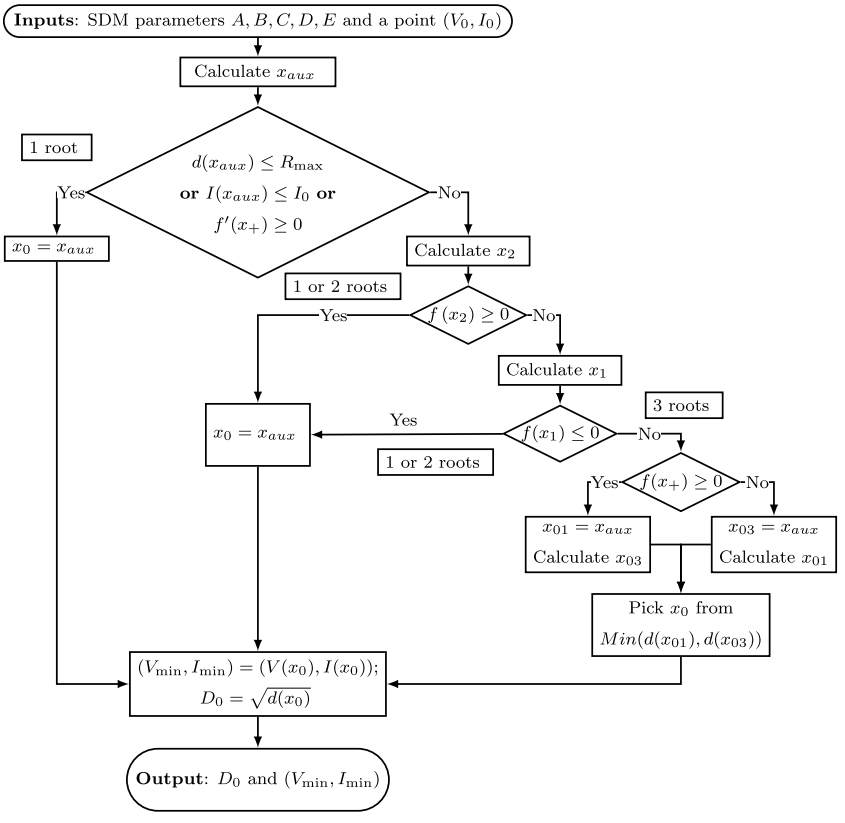

Fig. 11. Flowchart of algorithm to compute the ED from a point to an I–V curve.

- f *has a unique root*: In the three following cases f has a unique root and, when x_{aux} provides the Euclidean distance:

  (a) $d\,(x_{aux}) \leq R_{\max}$: which means that (V_0, I_0) is close enough to the I–V curve
  (b) $I\,(x_{aux}) \leq I_0$: which means that (V_0, I_0) is above the I–V curve
  (c) $f'\,(x_+) \geq 0$: which means that (V_0, I_0) is above the line $f'\,(x_+) = 0$

  In these cases, the point (V_0, I_0) is inside one of the following regions in Fig. 8: yellow, blue or green.

- *f has one or two roots*: If none of the previous cases are satisfied, one has in particular that $f'(x_+) < 0$ that guarantees the existence of x_1 and x_2 (roots of f'), which must be calculated (see in Appendix B.2 how to obtain these roots). Then, in the two following cases f has 1 or 2 roots and, again, x_{aux} provides the Euclidean distance:

  (a) $f(x_2) \geq 0$: the point (V_0, I_0) is in the blue region on the evolute of Fig. 8.
  (b) $f(x_1) \leq 0$: the point (V_0, I_0) is in the green region on the evolute of Fig. 8.

- *f has three roots*: In the remaining case, the point (V_0, I_0) is in the red region and, f has 3 roots. The Euclidean distance is obtained by comparing the two relative minima obtained with the seeds selection.

Comment: In the case $f'(x_+) < 0$, the roots x_1 and x_2 of the function $f'(x) = \frac{1}{x}\left(\beta x \ln x + 2\gamma x^2 + (\beta + \eta)\, x + \alpha\right)$, will be obtained through the solutions of the equation $fp(x) = 0$ where

$$fp(x) = \beta x \ln x + 2\gamma x^2 + (\beta + \eta)\, x + \alpha$$

5. Experimental results

As already discussed, the problem of obtaining the Euclidean distance from a point to a curve is, in general, a very hard mathematical problem. In our case, in addition, one has the burden that the I–V curve is given by an implicit equation, which implies that it is very challenging to compare our method with other counterparts in the literature. We have identified two methods from the state of the art that provide the Euclidean distance, although we will show that they fail under certain conditions. It should be emphasized that these special conditions are not generally known a priori and, therefore, the universal use of these methodologies could lead to erroneous results not being detected.

5.1. A system of two equations with two unknowns (S2E)

A sensible methodology to calculate the candidates to attain the Euclidean distance from a point (V_0, I_0) to the I–V curve given by (2) is obtained as follows. This formulation is based on [8] but using the parameters A, B, C, D, and E given in (3) used to rewrite the SDM equation as (2).

Since I is a differentiable function of V (see [42]), the optimization problem (12) is reduced to minimization of the one-variable function

$$F(V) = (V - V_0)^2 + (I - I_0)^2$$

where $I = I(V)$. The necessary condition for relative extremes (Fermat condition) $F'(V) = 0$ leads to the relation

$$I' = -\frac{V - V_0}{I - I_0} \tag{17}$$

Now, since

$$I' = -E - BC^V D^I \left(\ln C + I' \ln D\right) \tag{18}$$

one obtains from (17) and (18) the following expression as a necessary condition for relative extremes

$$V_0 - V - (I_0 - I)\, E - BC^V D^I \left((I_0 - I) \ln C - (V_0 - V) \ln D\right) = 0 \tag{19}$$

This relation (seen as a two-variables equation) together with the model Eq. (2) lead to the following system of two equations with two unknowns, whose solutions provide the candidate solutions to the optimization problem (12)

$$\begin{cases} I = A + B - EV - BC^V D^I \\ V_0 - V - (I_0 - I)\, E - BC^V D^I \left((I_0 - I) \ln C - (V_0 - V) \ln D\right) = 0 \end{cases} \tag{20}$$

This system can be solved, for example, with a numerical method like the Newton–Raphson method for systems of non-linear equations. It is well known that the N-R method converges if the seed is close enough to the solution and, moreover, we have seen in the previous section that if the point (V_0, I_0) is close enough to the I–V curve, then the solution of the problem (12) is unique. Therefore, if the point (V_0, I_0) itself is taken as seed so that the

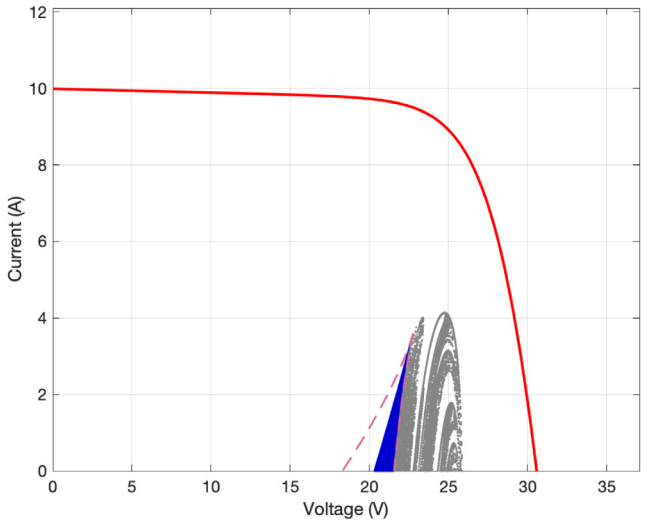

Fig. 12. Graphical representation of the regions where S2E method does not converge (gray) or it converges to a root different from the global minimum (blue).

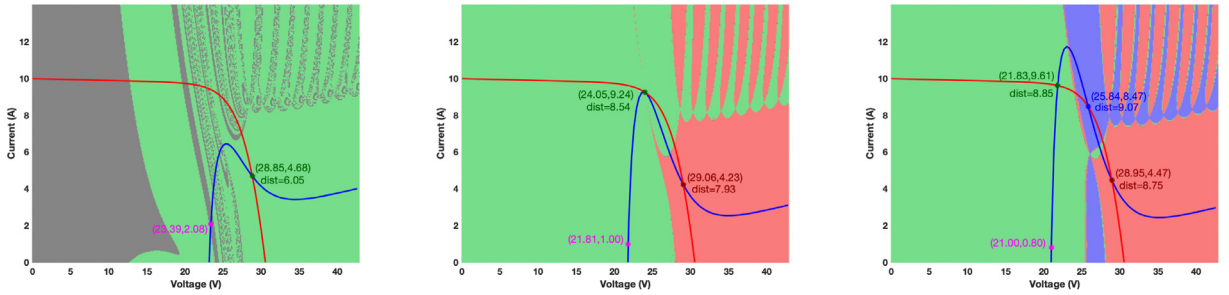

(a) 1 solution (b) 2 solutions (c) 3 solutions

Fig. 13. Graphical representation of the basins of attraction of the N-R method for the different possibilities of solutions of (20).

two previous closeness conditions are simultaneously satisfied, then the N-R method will provide the Euclidean distance. Let us call S2E the procedure of solving the system (20) with the N-R method taking (V_0, I_0) as seed.

Fig. 12 shows an example (SDM I–V curve with parameters $I_{ph} = 10A$, $I_s = 10^{-6}A$, $a = 1.9$, $R_s = 0.1\ \Omega$, $R_{sh} = 100\ \Omega$) where the system (20) is solved by the N-R method for a mesh of 2000 × 2000 points (V_0, I_0) distributed uniformly on the square image using each point itself as seed. The I–V curve is drawn in red; the points drawn in blue indicate seeds the N-R method converges to a solution where the Euclidean distance is not attained; in the gray points the N-R method does not converge at all; and in the remaining points (no color) N-R successfully identifies the correct solution. Please note that this analysis has been possible by comparing the N-R method results with the ones obtained by our method by means of distance tolerance of 10^{-12}. For the N-R method, a convergence tolerance of 10^{-12} and a maximum of 200 iterations are used, i.e. non-convergence is inferred by reaching the maximum number of iterations.

To better understand the behavior of the N-R method applied to system (20), Fig. 13 shows the basins of attraction of each solution in the three different possible cases, that is, when the system (20) has 1, 2 or 3 solutions. I–V curve is drawn in red and the blue curve represents the solutions of the necessary condition Eq. (19). Point (V_0, I_0) is drawn in purple and obviously lies into the blue curve. The color of each solution and the corresponding basin of attraction is the same. In gray color are shown the points/seeds for which the N-R method does not converge.

The fractal structure of each one of the basins of attraction must be emphasized, which explains the difficulty in selecting the seed for the N-R method. In addition, the point (V_0, I_0) itself is not always on the basin of attraction

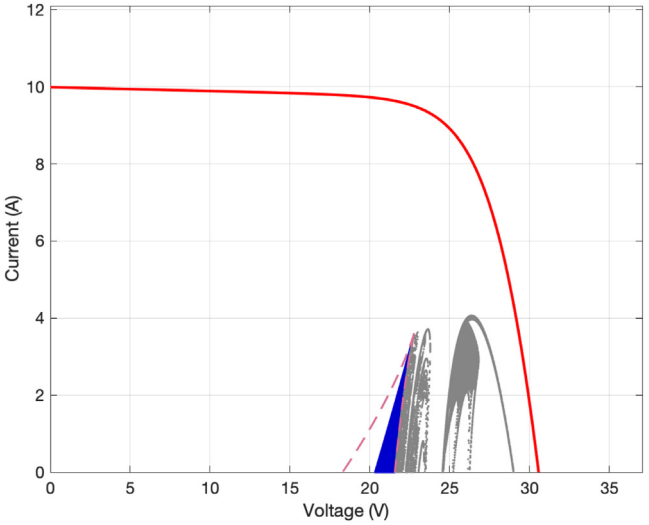

Fig. 14. Graphical representation of the regions where DVE method does not converge (gray) or it converges to a root different from the global minimum (blue).

of the solution corresponding to the Euclidean distance as shown above and occurs in practice during a parameter identification process via a curve fitting method.

5.2. The diode voltage equation (DVE)

In [8], the following alternative methodology was proposed to obtain the Euclidean distance under certain special hypotheses. Using the necessary condition for relative extremes (17) and the derivative expression (18) in terms of the original parameters, one obtains the one-variable equation

$$(I_{ph}-I_s(e^{\frac{V_D}{a}}-1)-\frac{V_D}{R_{sh}}-I_0)(R_s+(1+R_s^2)(\frac{1}{R_{sh}}+\frac{I_s}{a}e^{\frac{V_D}{a}}))-(V_D-V_0-I_0R_s)(1+R_s(\frac{1}{R_{sh}}+\frac{I_s}{a}e^{\frac{V_D}{a}}))=0 \quad (21)$$

where the unknown is the so-called *diode voltage* given by $V_D = V + IR_s$. Once the equation is solved, the corresponding point (V, I) given by

$$I = I_{ph} - I_s(e^{\frac{V_D}{a}} - 1) - \frac{V_D}{R_{sh}}$$
$$V = V_D - IR_s$$

is a candidate to attain the Euclidean distance. Observe that (21) is a nonlinear equation that can be solved by a numerical method. If one uses the N-R method with seed $V_D^{seed} = V_0 + I_0R_s$, one has that if (V_0, I_0) is close enough to the I–V curve to guarantee both, the solution of (12) is unique and the N-R method converges, then the obtained solution provides the Euclidean distance. In other case, this methodology does not provide the desired solution as we will see below with an analogous study to that performed for S2E. Let us call DVE the procedure of solving (21) with the N-R method taking $V_D^{seed} = V_0 + I_0R_s$ as seed.

Conclusions are similar to that obtained for S2E: if the seed V_D^{seed} is taken with the point (V_0, I_0) itself, there are points where the N-R method does not converge to the Euclidean distance, as seen in Fig. 14. Moreover, again the complicated structure of the basins of attraction of each solution indicates the difficulty to select the correct seed to the N-R method converges to the corresponding solution. As an example, a gray point has been taken from Fig. 14 and used as the nominal point (V_0, I_0) in the example represented in Fig. 15(a), where there is only one possible solution to be the Euclidean distance. As shown, (V_0, I_0) falls outside the basin of attraction of the N-R method and, therefore, the method does not converge taking this point as a seed. In the examples of Figs. 15(b) and 15(c), the DVE method converges to a solutions which do not provide the Euclidean distance.

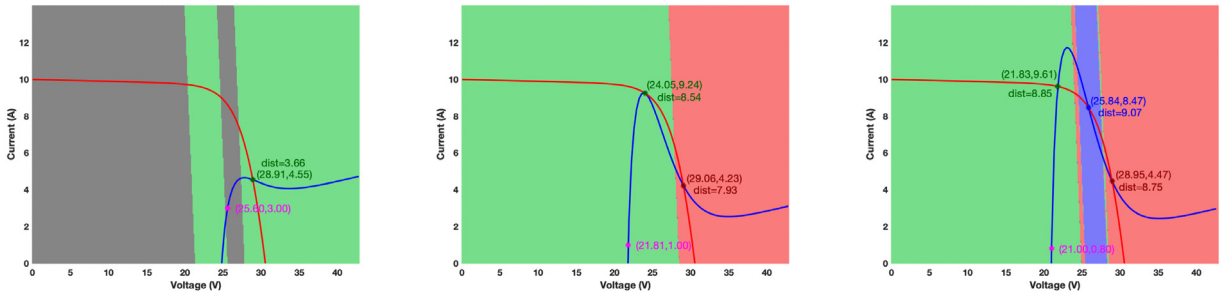

(a) 1 solution (b) 2 solutions (c) 3 solutions

Fig. 15. Graphical representation of the basins of attraction of the N-R method for the different possibilities of solutions of (21).

Table 1
Execution times and failures obtained for S2E, DVE and ED.

Methods	Time (s)			Failures		
Noise Level	Low	Medium	High	Low	Medium	High
S2E	0.20013	0.20522	0.23397	0%	0%	0.38%
DVE	0.064051	0.063244	0.067489	0%	0%	2.27%
ED	0.046947	0.045734	0.048097	0%	0%	0%

5.3. Experimental results with noisy points of an I–V curve

One of the main applications of the calculus of the Euclidean distance from a point to an I–V curve is to perform orthogonal distance regression (ODR) to obtain the best fit of an I–V curve based on the PV SDM to a set of experimental noisy points (V_i^{exp}, I_i^{exp}). This is equivalent to finding the 5 parameters of the SDM I–V curve that minimize the objective function (22)

$$S_{ED} = \sum_{i=1}^{N} (V_i^{exp} - V_i^{theo})^2 + (I_i^{exp} - I_i^{theo})^2 \tag{22}$$

where (V_i^{theo}, I_i^{theo}) is a point of the I–V curve closest (in the Euclidean distance sense) to (V_i^{exp}, I_i^{exp}), for each $i = 1, \ldots, N$, with N being the number of samples. This type of optimization procedure is a better option (see [8]) than the ordinary linear regression to obtain the maximum likelihood estimation (MLE) of the SDM parameters when there is noise in both, the voltage and the current of the samples.

As we have seen in the previous subsections, if the points are not sufficiently close to the I–V curve to ensure unicity in the solution and convergence of the N-R method, the previous methodologies S2E and DVE may fail to find the Euclidean distance and be inappropriate to perform ODR without additional interventions.

Let us see what happens in one example where three different levels of Gaussian noise with standard deviations ($\sigma \in \{0.001, 0.01, 0.1\}$) and weighted by V_{OC} in voltage noise and I_{SC} in current noise, are added to 1000 samples of a synthetic I–V curve with the same parameters as in Section 5.1. As before, the proposed method hereinafter denoted as ED (from Euclidean Distance) is used as a benchmark to assess whether S2E and DVE successfully obtain the Euclidean distance and capture their execution cost (average of 100 repetitions). Results are shown in Table 1.

As expected from the aforementioned theoretical analysis, if the noise is low or medium, the noisy points are sufficiently near to the I–V curve to satisfy the proximity conditions which ensure that S2E and DVE methods attain the Euclidean distance. However, when noise is high, these methods fail in some cases. Nevertheless, the execution time is always higher than ED, despite all the necessary casuistry performed in the latter. This indicates that the sophisticated ED design not only guarantees universal convergence to the right solution, but it does it also at the most computationally efficient way. Between S2E and DVE, the latter is faster due to the 1-equation formulation, but it fails more often.

Table 2
Results for the ODR using S2E, DVE or ED.

Methods	Time (s)			Failures			Best RMSE		
Noise Level	Low	Medium	High	Low	Medium	High	Low	Medium	High
S2E	2.6235	10.686	8.7305	0%	0%	6%	44%	13%	7%
DVE	0.85821	3.4582	3.9172	0%	0%	15%	41%	9%	3%
ED	0.47458	3.0602	3.4956	0%	0%	0%	100%	100%	100%

Table 3
Sets of basic seeds for ODR initialization.

Name/Parameters	I_{ph} (A)	I_{sat} (A)	n	$R_s = 1$ (Ω)	$R_{sh} = 1$ (Ω)
ONES	1	1	1	1	1
NMO	1	10^{-6}	1	1	10^3
TSLLS1	I_{ph}^{TSLLS1}	I_{sat}^{TSLLS1}	R_s^{TSLLS1}	R_{sh}^{TSLLS1}	I_{ph}^{TSLLS1}

To better understand the practical impact of the ED algorithm, we have taken a set of 200 noisy points from an I–V curve with the levels of noise indicated previously and then performed an ODR to obtain the parameters of the SDM where the original parameters have been used to initialize the regression procedure. The `lsqnonlin` MATLAB function has been used in all implementations with the same convergence tolerances. Again, in order to obtain a reliable and stable execution time, the average of 100 repetitions of each experiment has been taken.

In the case of high noise, the methods S2E and DVE fail at some instances as shown in Table 2, that is, the `lsqnonlin` function has returned error and the ODR process could not be completed; on the contrary, with the ED algorithm all the ODR executions were entirely successful. For low and medium levels of noise, all the methods have converged and provided practically the same SDM parameters but, as it happened for the synthetic curves, the ED algorithm has been the fastest as can be seen in Table 2. As expected, execution times increase when noise level is higher because more iterations for the Newton–Raphson method convergence are needed. Again, DVE is faster than 2SE but suffers from more failures.

The third column group of Table 2 provides the best Root Mean Square Error (RMSE) with respect to the Euclidean distance given by $RMSE = \sqrt{\frac{1}{N} S_{ED}}$, where S_{ED} is given in (22) and the theoretical points are obtained with the ED method. Thus, for each simulation, we have calculated the corresponding RMSE and we have considered that a simulation reaches the best RMSE if it differs from the lowest by less than 10^{-9}. Although this output should not be significant when the ODR successfully completes, since all the methods only act as internal loops to obtain the Euclidean distances, it is worth noting that only with the ED method the best RMSE is obtained 100% of the times. With the other methods, the RMSE is less than optimal quite often, being worse at higher noise levels. This further confirms the accuracy and robustness of the ED algorithm.

5.4. Validation on the NREL dataset

To evaluate the benefits of the ED algorithm in real cases, the ODR has been performed on a selection of I–V curves taken from the National Renewable Energy Laboratory (NREL) dataset [34], measured from the mSi460A8 panel at the Cocoa location. Specifically, 1000 curves have been randomly selected and no parameters such as irradiance or temperature have been filtered. As in the previous subsection, we have used S2E, DVE and ED as internal loops to compute the Euclidean distance in the ODR. Since the initial parameters are very important in ODR, we have also used three basic sets of seeds given in Table 3 where NMO (Normal Magnitude Order) is a selection of orders of magnitude that could be found in parameters of I–V curves measured under non-extreme environmental conditions and with panels that are not too degraded. Parameters corresponding of TSLLS1 are those obtained with the first phase of the TSLLS method [44] (see https://pvmodel.umh.es/) which would generally be close to the ODR solution (see [8]).

Similar to the previous subsection, Table 4 shows that ODR falls in some cases when methods S2E and DVE are used as internal loops to compute the Euclidean distance, while it always works fine with the ED algorithm. But what is striking again is that the best RMSE is attained 100% of the times only with the ED algorithm in contrast

Table 4
ODR using S2E, DVE and ED in 1000 I–V curves from NREL dataset.

Seeds	ONES			NMO			TSLLS1		
	Best RMSE	RMSE<0.01	Failures	Best RMSE	RMSE<0.01	Failures	Best RMSE	RMSE<0.01	Failures
S2E	9.4%	3.2%	0.4%	6.2%	26.5%	0%	19.8%	99.2%	0%
DVE	9.8%	2.7%	3.5%	7.0%	26.5%	1%	7.6%	99.2%	0%
ED	100%	26.1%	0%	100%	84.2%	0%	100%	99.3%	0%

to the other two counterparts. Please also observe that when TSLLS1 parameters are used as seeds, none of the methods fails, and this is also almost the case with NMO parameters since the produced I–V curves happen to be sufficiently close to the samples that feature limited only noise. In Table 4, we have added as extra information the percentage of times that the RMSE is smaller than a small quantity (for example 0.01) when the three methods to compute the Euclidean distance are used in the ODR. At all noise levels, the best method to obtain an RMSE smaller than 0.01 is the ED algorithm, being almost the same when the initial seeds are close to the final solution, which again indicates the benefit of ED over the other methods for any seed selection.

6. Conclusion

In this paper we provide a new parametrization of the single-diode model I–V curve. This parametrization allows reducing the calculus of the Euclidean distance from a point to an I–V curve to solve a single variable equation. A deep analytical study of the function involved in this equation provides a complete casuistry of all possible solutions, performed for the first time. A geometrical study based on the curvature of the I–V curve as well as the Maximum Curvature Point has allowed to design an optimized algorithm (Algorithm 1) which computes with high speed and accuracy the Euclidean distance from a point to an I–V curve without failures. The proposed method has been compared with a couple of methods available in literature (S2E and DVE) for solving this problem in special conditions which ensure their convergence. The consistency and reliability of the proposed method ED has been proved and its performance is the best between the methods compared. As a main conclusion, the proposed method is found as the only reliable method with the best performance for calculating the Euclidean distance from a point to the I–V curve of the SDM model and allows the possibility of performing a robust orthogonal distance regression without failures.

Acknowledgments

Dr. F. Javier Toledo, Dr. V. Galiano, Dr. Victoria Herranz and Dr. José M. Blanes have received funding from grant TED2021-130025B-I00 funded by MCIN/AEI/10.13039/501100011033 and by the European Union NextGenerationEU/PRTR. Dr. F. Javier Toledo's work has received funding from the Ministerio de Ciencia e Innovación of Spain (PGC2018-097960-B-C21), the government of the Valencian Community (PROMETEO/2021/063) and the European Union (ERDF, "A way to make Europe"). Dr. V. Galiano's work has received funding from the Valencian Ministry of Innovation, Universities, Science and Digital Society (Generalitat Valenciana) under Grant CIAICO/2021/278 and from Grant PID2021-123627OB-C55 funded by MCIN/AEI/ 10.13039/501100011033 and, by "ERDF A way of making Europe". Dr. E. Batzelis' work has received funding from the Royal Academy of Engineering under the Engineering for Development Research Fellowship scheme (number RF/201819/18/86).

Appendix A. ED algorithm pseudocode

See Algorithm 1.

Algorithm 1: Pseudocode of the Euclidean distance method

Input: SDM parameters A, B, C, D, E and a point (V_0, I_0)

Output: Euclidean distance, D_0, from the point (V_0, I_0) to the I-V curve $I = A + B - EV - BC^V D^I$, and the $(V_{\min}, I_{\min})$ where the distance is attained

Notation : $NR(f; x_s)$ means Newton–Raphson method to compute the root of f starting from the seed x_s $RF(fp; 0^+, x_+)$ means Regula-Falsi type method to compute the root of fp in the interval $]0^+, x_+]$

Define $f(x)$; $f'(x)$; $fp(x)$; $d(x)$; $V(x)$; $I(x)$; x_+; $R_{\max}$; α; β; γ; δ; η; ρ; $u = \min\{1, x_+\}$;
if $f(x_+) \geq 0$ **then**
  $x_s = \min\{1, \exp(-\frac{\gamma u^2 + \max\{0, \eta\}u + \rho}{\alpha})\}$;
else
  $x_s = \max\{1, \frac{-\eta + \sqrt{\max\{0, \eta^2 - 4\gamma\rho\}}}{2\gamma}\}$; `// seed for` x_{aux}

Initialización Phase

$x_{aux} = NR(f; x_s)$;
if $d(x_{aux}) \leq R_{\max}$ ***or*** $I(x_{aux}) \leq I_0$ ***or*** $f'(x_+) \geq 0$ **then**
  $x_0 = x_{aux}$;
else

1 root of f

  $x_s = \max\{1, \frac{-(\beta + \eta) + \sqrt{\max\{0, (\beta + \eta)^2 - 8\gamma\alpha\}}}{4\gamma}\}$ `// seed for` x_2
  $x_2 = NR(fp; x_s)$; `// computation of` x_2
  if $f(x_2) \geq 0$ **then** `//` $f(x_2) \geq 0$ `implies` $f(x_+) \geq 0$
    $x_0 = x_{aux}$;
  else
    $x_1 = RF(fp; 0^+, x_+)$; `// computation of` x_1
    if $f(x_1) \leq 0$ **then** `//` $f(x_1) \leq 0$ `implies` $f(x_+) \leq 0$
      $x_0 = x_{aux}$;
    else

1 or 2 roots of f

      if $f(x_+) \geq 0$ **then**
        $x_{01} = x_{aux}$;
        $x_s = \max\{1, \frac{-\eta + \sqrt{\max\{0, \eta^2 - 4\gamma\rho\}}}{2\gamma}\}$; `// seed for` x_{03}
        $x_{03} = NR(f; x_s)$; `// computation of` x_{03}
      else
        $x_{03} = x_{aux}$;
        $x_s = \min\{1, \exp(-\frac{\gamma u^2 + \max\{0, \eta\}u + \rho}{\alpha})\}$; `// seed for` x_{01}
        $x_{01} = NR(f; x_s)$; `// computation of` x_{01}
      if $d(x_{01}) \leq d(x_{03})$ **then**
        $x_0 = x_{01}$;`// in the case` $d(x_{01}) = d(x_{03})$ `choose` x_{01}
      else
        $x_0 = x_{03}$;

3 roots of f

$(V_{\min}, I_{\min}) = (V(x_0), I(x_0))$;
$D_0 = \sqrt{d(x_0)}$;

Appendix B. Roots computation

B.1. Seeds to initialize the Newton–Raphson method to find the roots of f in the ED algorithm.

Recall that

$$f(x) = (\alpha + \beta x)\ln x + \gamma x^2 + \eta x + \rho, \quad \text{with } \alpha, \beta, \gamma > 0.$$

Let us distinguish the following two cases:

(a) $f(x_+) \geq 0$

To find the largest root in the subcase $f'(x_+) < 0$ with $f(x_1) > 0$ and $f(x_2) < 0$, we will use the same procedure explained later in the case $f(x_+) < 0$. Now we look for the smallest root $x_{\min}$ of f.

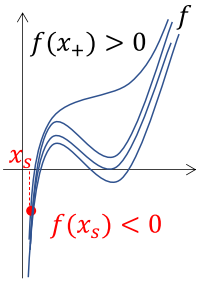

Fig. B.16. Possible graphs of f in the case $f(x_+) \geq 0$..

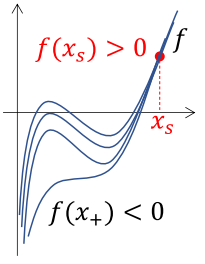

Fig. B.17. Possible graphs of f in the case $f(x_+) < 0$..

The Newton–Raphson method initialized from a seed x_s in the interval $]0, x_{\min}]$ will converge to $x_{\min}$. To obtain x_s, we want to find a continuous function above f in the interval $]0, x_{\min}]$, as close as possible to f, and with a root easy to compute. This root will be the seed x_s (see Fig. B.16). The idea is that f is close to $\alpha \ln x + c$ for small positive values of x, where c is a constant only depending on the parameters and (V_0, I_0).

- If $x_+ \leq 1$, for $0 < x \leq x_+$, one has $\ln x \leq 0$ and

$$f(x) < \alpha \ln x + \gamma x_+^2 + \max\{0, \eta\} x_+ + \rho$$
$$= \underbrace{\alpha \ln x + \gamma (\overbrace{\min\{1, x_+\}}^{u})^2 + \max\{0, \eta\} \overbrace{\min\{1, x_+\}}^{u} + \rho}_{g(x)}$$

  Since $0 < x_{\min} \leq x_+$, the unique root of g given by

$$\exp(-\frac{\gamma u^2 + \max\{0, \eta\} u + \rho}{\alpha})$$

  belongs to $]0, x_{\min}[$.
- If $x_+ > 1$, we distinguish the following cases:
  - If $f(1) \leq 0$, then $1 \in]0, x_{\min}]$.
  - If $f(1) > 0$, then $x_{\min} < 1$ and $\ln x < 0$ for $0 < x \leq x_{\min}$, which implies for these values of x that

$$f(x) < g(x)$$

    and, the unique root of g belongs to $]0, x_{\min}[$.

Therefore, the following seed guarantees that the Newton–Raphson method applied to f converges to $x_{\min}$

$$x_s = \min\{1, \exp(-\frac{\gamma u^2 + \max\{0, \eta\} u + \rho}{\alpha})\} \in]0, x_{\min}]$$

(b) $f(x_+) < 0$

To find the smallest root in the subcase $f'(x_+) < 0$ with $f(x_1) > 0$ and $f(x_2) < 0$, we will use the same procedure explained before in the case $f(x_+) \geq 0$. Now we look for the largest root $x_{\max}$ of f.

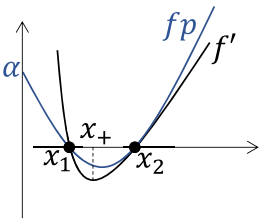

Fig. B.18. Graphs of f' and fp.

The Newton–Raphson method initialized from a seed x_s in the interval $[x_{\max}, +\infty[$ will converge to $x_{\max}$. To obtain x_s, we want to find a continuous function below f in the interval $[x_{\max}, +\infty[$, as close as possible to f, and with a root easy to compute. This root will be the seed x_s (see Fig. B.17). The idea is that f is close to the parabola $\gamma x^2 + \eta x + \rho$ (recall $\gamma > 0$) for large values of x.

- If $x_+ \geq 1$, for $x \geq x_+$ one has $\ln x \geq 0$ and

$$\gamma x^2 + \eta x + \rho < \underbrace{(\alpha + \beta x)\ln x + \gamma x^2 + \eta x + \rho}_{f(x)}$$

  Since $x_{\max} \geq x_+$, the maximum root of $\gamma x^2 + \eta x + \rho$ given by

$$\frac{-\eta + \sqrt{\eta^2 - 4\gamma\rho}}{2\gamma}$$

  belongs to $[x_{\max}, +\infty[$.
- If $x_+ < 1$, we distinguish the following cases:
  - If $f(1) \geq 0$, then $1 \in [x_{\max}, +\infty[$.
  - If $f(1) < 0$, then $x_{\max} > 1$. Since $\ln x > 0$ for $x > 1$, one has

$$\gamma x^2 + \eta x + \rho \leq f(x) \text{ for } x > 1$$

    and, as before,

$$\frac{-\eta + \sqrt{\eta^2 - 4\gamma\rho}}{2\gamma} \in [x_{\max}, +\infty[$$

Therefore, the seed x_s given by

$$x_s = \max\{1, \frac{-\eta + \sqrt{\max\{0, \eta^2 - 4\gamma\rho\}}}{2\gamma}\} \in [x_{\max}, +\infty[$$

guarantees that the Newton–Raphson method applied to f converges to $x_{\max}$.

Note: The use of $\frac{1}{2\gamma}(-\eta + \sqrt{\max\{0, \eta^2 - 4\gamma\rho\}})$ instead of $\frac{1}{2\gamma}(-\eta + \sqrt{\eta^2 - 4\gamma\rho})$ avoid complex numbers when $\gamma x^2 + \eta x + \rho$ has no real roots in the case $f(1) \geq 0$.

B.2. Finding the roots of fp in the ED algorithm.

Now we want to obtain the roots x_1 and x_2 of $f'(x) = \frac{1}{x} fp(x)$ in the case $f'(x_+) < 0$ with $f(x_1) > 0$ and $f(x_2) < 0$, which is the same to find the roots of fp where

$$fp(x) = \beta x \ln x + 2\gamma x^2 + (\beta + \eta)x + \alpha$$

(see Fig. B.18).

- Since $fp(0^+) = \lim_{xarrow0^+} fp(x) = \alpha > 0$ and $fp(x_+) < 0$, to compute the root x_1 of fp it is used a Regula-Falsi type method defined by the following iterative scheme $z_{k+1} = \dfrac{\alpha z_k}{\alpha - fp(z_k)}$ with $z_0 = x_+$.

Another possibility is to use the N-R method with a seed obtained with the following strategy: Start with a small positive $x_s < x_+$ (for example $x_s = \frac{x_+}{10}$) and compute $fp(x_s)$. If $fp(x_s) = 0$ then $x_1 = x_s$. If $fp(x_s) > 0$ apply Newton–Raphson method to compute the root of fp. If $fp(x_s) < 0$, do $x_s = \frac{x_s}{10}$ (10 can be changed for any number greater than 1) and start again. This last strategy can be used indeed to obtain all the seeds in the ED algorithm.

- To obtain the root x_2, we proceed similarly to the largest root of f. Now, we want to apply the Newton–Raphson method to fp with a seed x_s in the interval $[x_2, +\infty[$ that ensures convergence to x_2. To obtain x_s, we want to find a continuous function below fp in the interval $[x_2, +\infty[$, as close as possible to fp, and with a root easy to compute. The idea followed now is that fp is close to the parabola $2\gamma x^2 + (\beta + \eta)x + \alpha$ (recall $\gamma > 0$) for large values of x. The seed x_s obtained with the procedure previously discussed (even with the same casuistry but applied to fp) is

$$x_s = \max\{1, \frac{-(\beta + \eta) + \sqrt{\max\{0, (\beta + \eta)^2 - 8\gamma\alpha\}}}{4\gamma}\}$$

which guarantees that the Newton–Raphson method applied to fp converges to x_2.

Appendix C. Some calculus developments

C.1.

Let us see that

$$d'(x) = \frac{2}{\delta^2 x}(\underbrace{(\alpha + \beta x)\ln x + \gamma x^2 + \eta x + \rho)}_{f(x)}$$

where

$$\begin{aligned}
\alpha &= 1 + E^2 \\
\beta &= \ln D + E \ln C \\
\gamma &= (\ln C)^2 + (\ln D)^2 \\
\delta &= \ln C - E \ln D \\
\eta &= \beta(1 - \ln B) - \gamma(A + B) + \delta(I_0 \ln C - V_0 \ln D) \\
\rho &= -(\alpha \ln B + \beta(A + B) + \delta(V_0 - E I_0))
\end{aligned}$$

Recalling that

$$d(x) = (\mathcal{V}(x) - V_0)^2 + (\mathcal{I}(x) - I_0)^2$$

with

$$\begin{cases} \mathcal{V}(x) = \frac{1}{\delta}(\ln x - (A + B - x)\ln D - \ln B) \\ \mathcal{I}(x) = A + B - E\mathcal{V}(x) - x \end{cases}$$

one has that

$$\begin{aligned}
d'(x) &= 2(\mathcal{V}(x) - V_0)\mathcal{V}'(x) + 2(\mathcal{I}(x) - I_0)\mathcal{I}'(x) = \\
&= 2(\underbrace{\frac{1}{\delta}(\ln x - (A + B - x)\ln D - \ln B)}_{\mathcal{V}(x)} - V_0)\underbrace{\frac{1}{\delta}(\frac{1}{x} + \ln D)}_{\mathcal{V}'(x)} \\
&+ 2(\underbrace{A + B - E\overbrace{\frac{1}{\delta}(\ln x - (A + B - x)\ln D - \ln B)}^{\mathcal{V}(x)} - x}_{\mathcal{I}(x)} - I_0)(\underbrace{-E\overbrace{\frac{1}{\delta}(\frac{1}{x} + \ln D)}^{\mathcal{V}'(x)} - 1}_{\mathcal{I}'(x)})
\end{aligned}$$

$$
\begin{aligned}
&= \frac{2}{\delta^2}((\ln x - (A+B-x)\ln D - \ln B - \delta V_0)(\frac{1}{x} + \ln D) \\
&+ (\delta(A+B) - E(\ln x - (A+B-x)\ln D - \ln B) - \delta x - \delta I_0)(-E(\frac{1}{x} + \ln D) - \delta)) \\
&= \frac{2}{\delta^2 x}((\ln x - (A+B-x)\ln D - \ln B - \delta V_0)(1 + x\ln D) \\
&+ (\delta(A+B) - E(\ln x - (A+B-x)\ln D - \ln B) - \delta x - \delta I_0)(-E(1 + x\ln D) - \delta x)) \\
&= \frac{2}{\delta^2 x}((1 + x\ln D - E(-E - x(\underbrace{E\ln D + \delta}_{\ln C})))\ln x \\
&+ ((\ln D)^2 + (\underbrace{E\ln D + \delta}_{\ln C})^2)x^2 \\
&+ (\ln D - ((A+B)\ln D + \ln B + \delta V_0)\ln D + (\underbrace{E\ln D + \delta}_{\ln C})E \\
&+ ((A+B)(\underbrace{E\ln D + \delta}_{\ln C}) + E\ln B - \delta I_0)(\underbrace{-E\ln D - \delta}_{-\ln C}))x \\
&+ (-(A+B)\ln D - \ln B - \delta V_0 + (\delta(A+B) + E(A+B)\ln D + E\ln B - \delta I_0)(-E))) \\
&= \frac{2}{\delta^2 x}((\underbrace{1+E^2}_{\alpha} + (\underbrace{\ln D + E\ln C}_{\beta})x)\ln x \\
&+ (\underbrace{(\ln D)^2 + (\ln C)^2}_{\gamma})x^2 \\
&+ ((\underbrace{\ln D + E\ln C}_{\beta})(1 - \ln B) - (A+B)(\underbrace{(\ln D)^2 + (\ln C)^2}_{\gamma}) + \delta(I_0\ln C - V_0\ln D))x \\
&- \delta(V_0 - I_0 E) - (A+B)(\underbrace{\ln D + E(\overbrace{\delta + E\ln D}^{\ln C})}_{\beta}) - \ln B(\underbrace{1+E^2}_{\alpha})) \\
&= \frac{2}{\delta^2 x}((\alpha + \beta x)\ln x + \gamma x^2 + \eta x + \rho) = \frac{2}{\delta^2 x} f(x)
\end{aligned}
$$

C.2.

Let us see that

$$k(x) = \frac{\delta^2 x}{(\gamma x^2 + 2\beta x + \alpha)^{3/2}}$$

Recall that the curvature of the function I is given by the formula

$$k = \frac{|I''|}{(1 + (I')^2)^{3/2}} = \frac{-I''}{(1 + (I')^2)^{3/2}} \tag{C.1}$$

and also recall the relations

$$I'' = \frac{(\ln C + I'\ln D)^2}{\ln C - E\ln D}(I' + E) \text{ and } I' = -\frac{E + x\ln C}{1 + x\ln D}$$

Then

$$
\begin{aligned}
k(x) &= \frac{-I''}{(1 + (I')^2)^{3/2}} = -\frac{\frac{(\ln C + I'\ln D)^2}{\ln C - E\ln D}(I' + E)}{(1 + (I')^2)^{3/2}} = -\frac{(\ln C + I'\ln D)^2(I' + E)}{(\ln C - E\ln D)(1 + (I')^2)^{3/2}} \\
&= -\frac{(\ln C - \frac{E + x\ln C}{1 + x\ln D}'\ln D)^2(-\frac{E + x\ln C}{1 + x\ln D} + E)}{(\ln C - E\ln D)(1 + (-\frac{E + x\ln C}{1 + x\ln D})^2)^{3/2}}
\end{aligned}
$$

$$
\begin{aligned}
&= -\frac{\frac{1}{(1+x\ln D)^3}((1+x\ln D)\ln C-(E+x\ln C)\ln D)^2(-(E+x\ln C)+E(1+x\ln D))}{\frac{1}{(1+x\ln D)^3}(\ln C-E\ln D)((1+x\ln D)^2+(E+x\ln C)^2)^{3/2}}\\
&= -\frac{(\ln C+x\ln D\ln C-E\ln D-x\ln C\ln D)^2(-E-x\ln C+E+xE\ln D)}{(\ln C-E\ln D)((1+x\ln D)^2+(E+x\ln C)^2)^{3/2}}\\
&= -\frac{(\ln C-E\ln D)^2(-x(\ln C-E\ln D))}{(\ln C-E\ln D)((1+x\ln D)^2+(E+x\ln C)^2)^{3/2}}\\
&= \frac{(\ln C-E\ln D)^2x}{((1+x\ln D)^2+(E+x\ln C)^2)^{3/2}} = \frac{\delta^2x}{((1+x\ln D)^2+(E+x\ln C)^2)^{3/2}}\\
&= \frac{\delta^2x}{(1+x^2\ln^2 D+2x\ln D+E^2+x^2\ln^2 C+2xE\ln C)^{3/2}}\\
&= \frac{\delta^2x}{(\gamma x^2+2\beta x+\alpha)^{3/2}}
\end{aligned}
$$

C.3.

Let us see that the critical points of k (those where $k'=0$) are exactly the same points where $f''=0$.

$$
\begin{aligned}
k'(x) &= \frac{\delta^2(\alpha+2\beta x+\gamma x^2)^{3/2}-\delta^2x\frac{3}{2}(\alpha+2\beta x+\gamma x^2)^{1/2}(2\beta+2\gamma x)}{(\alpha+2\beta x+\gamma x^2)^3}\\
&= \frac{(\alpha+2\beta x+\gamma x^2)^{1/2}(\delta^2(\alpha+2\beta x+\gamma x^2)-3\delta^2x(\beta+\gamma x))}{(\alpha+2\beta x+\gamma x^2)^3}\\
&= \frac{\delta^2(\alpha+2\beta x+\gamma x^2)^{1/2}(\alpha+2\beta x+\gamma x^2-3x\beta-3\gamma x^2)}{(\alpha+2\beta x+\gamma x^2)^3}\\
&= \frac{-\delta^2(2\gamma x^2+\beta x-\alpha)}{(\alpha+2\beta x+\gamma x^2)^{5/2}}
\end{aligned}
$$

Then

$$k'(x)=0 \leftrightarrow 2\gamma x^2+\beta x-\alpha=0 \leftrightarrow f''(x)=0$$

References

[1] N.F. Abdul Hamid, N. Abdul-Rahim, J. Selvaraj, Solar cell parameters extraction using particle swarm optimization algorithm, in: IEEE Conference on Clean Energy and Technology, 2013, pp. 461–465, http://dx.doi.org/10.1109/CEAT.2013.6775676.

[2] M.F. AlHarjri, K.M. El-Naggar, M.R. AlRashidi, A.K. Al-Othman, Optimal extraction of solar cell parameters using pattern search, Renew. Energy 44 (2012) 238–245, http://dx.doi.org/10.1016/j.renene.2012.01.082.

[3] A. Askarzadeh, A. Rezazadeh, Parameter identification for solar cell models using harmony search-based algorithms, Sol. Energy 86 (2012) 3241–3249, http://dx.doi.org/10.1016/j.solener.2012.08.018.

[4] T.C. Banwell, A. Jayakumar, Exact analytical solution for current flow through diode with series resistance, ELectron. Lett. 36 (2000) 291–292, http://dx.doi.org/10.1049/el:20000301.

[5] J.D. Bastidas-Rodriguez, G. Petrone, C.A. Ramos-Paja, G. Spagnuolo, A genetic algorithm for identifying the single diode model parameters of a photovoltaic panel, Math. Comput. Simul. 131 (2017) 38–54, http://dx.doi.org/10.1016/j.matcom.2015.10.008.

[6] J. Bastidas-Rodriguez, G. Petrone, C. Ramos-Paja, G. Spagnuolo, Quantification of photovoltaic module degradation using model based indicators, Math. Comput. Simul. 131 (2017) 101–113, http://dx.doi.org/10.1016/j.matcom.2015.04.003.

[7] E. Batzelis, Simple PV performance equations theoretically well founded on the single-diode model, IEEE J. Photovolt. 7 (2017) 1400–1409, http://dx.doi.org/10.1109/JPHOTOV.2017.2711431.

[8] E. Batzelis, J.M. Blanes, F.J. Toledo, V. Galiano, Noise-scaled euclidean distance: A metric for maximum likelihood estimation of the PV model parameters, IEEE J. Photovolt. 12 (3) (2022) 815–826, http://dx.doi.org/10.1109/JPHOTOV.2022.3159390.

[9] E.I. Batzelis, S.A. Papathanassiou, A method for the analytical extraction of the single-diode PV model parameters, IEEE Trans. Sustain. Energy 7 (2) (2016) 504–512, http://dx.doi.org/10.1109/TSTE.2015.2503435.

[10] J.M. Blanes, F.J. Toledo, S. Montero, A. Garrigós, In-site real-time photovoltaic I-V curves and maximum power point estimator, IEEE Trans. Power Electron. 28 (2013) 1234–1240, http://dx.doi.org/10.1109/TPEL.2012.2206830.

[11] P.T. Boggs, R.H. Byrd, J.E. Donaldson, R.B. Schnabel, Algorithm 676: ODRPACK: Software for weighted orthogonal distance regression, ACM Trans. Math. Software 15 (1989) 1052–1078, http://dx.doi.org/10.1145/76909.76913.

[12] P.T. Boggs, R.H. Byrd, J.E. Rogers, R.B. Schnabel, User's reference guide for ODRPACK version 2.01:: software for weighted orthogonal distance regression, 1992.

[13] P.T. Boggs, R.H. Byrd, R.B. Schnabel, A stable and efficient algorithm for nonlinear orthogonal distance regression, SIAM J. Sci. Stat. Comput. 8 (1987) 1052–1078, http://dx.doi.org/10.1137/0908085.
[14] P.T. Boggs, J.E. Rogers, Orthogonal distance regression, Contemp. Math. 112 (1990) 183–194.
[15] M. Campanelli, B.H. Hamadani, Calibration of a single-diode performance model without a short-circuit temperature coefficient, Energy Sci. Eng. 6 (2018) 222–238, http://dx.doi.org/10.1002/ese3.190.
[16] A.A. Cárdenas, M. Carrasco, F. Mancilla-David, A. Street, R. Cárdenas, Experimental parameter extraction in the single-diode photovoltaic model via a reduced-space search, IEEE Trans. Ind. Electron. 64 (2) (2017) 1468–1476, http://dx.doi.org/10.1109/TIE.2016.2615590.
[17] C. Chellaswamy, R. Ramesh, Parameter extraction of solar cell models based on adaptive differential evolution algorithm, Renew. Energy 97 (2016) 823–837, http://dx.doi.org/10.1016/j.renene.2016.06.024.
[18] J.L. Coolidge, The unsatisfactory story of curvature, Amer. Math. Monthly 59 (6) (1952) 375–379, http://dx.doi.org/10.1080/00029890.1952.11988145.
[19] J. Cubas, S. Pindado, C. De Manuel, Explicit expressions for solar panel equivalent circuit parameters based on analytical formulation and the Lambert W-function, Energies 7 (2014) 4098–4115, http://dx.doi.org/10.3390/en7074098.
[20] W. De Soto, S.A. Klein, W.A. Beckman, Improvement and validation of a model for photovoltaic array performance, Sol. Energy 80 (1) (2006) 78–88, http://dx.doi.org/10.1016/j.solener.2005.06.010.
[21] M.C. Di Piazza, M. Luna, G. Petrone, G. Spagnuolo, Parameter translation for single-diode PV models based on explicit identification, in: 2017 IEEE International Conference on Environment and Electrical Engineering and 2017 IEEE Industrial and Commercial Power Systems Europe (EEEIC / I CPS Europe), Milan, Italy, 2017, pp. 1–5, http://dx.doi.org/10.1109/EEEIC.2017.7977773.
[22] T. Easwarkhanthan, J. Bottin, I. Bouhouch, C. Boutrit, Nonlinear minimization algorithm for determining the solar cell parameters with microcomputers, Int. J. Sol. Energy 4 (1) (1986) 1–12, http://dx.doi.org/10.1080/01425918608909835.
[23] K.M. El-Naggar, M.R. AlRashidi, M.F. AlHajri, A.K. Al-Othman, Simulated annealing algorithm for photovoltaic parameters identification, Sol. Energy 86 (2012) 266–274, http://dx.doi.org/10.1016/j.solener.2011.09.032.
[24] V. Hernandez-Mederos, J. Estrada-Sarlabous, P. Barrera-Sánchez, On the Euclidean distance from a point to a conic, Rev. Integr. Temas Mat. 15 (1) (1997) 45–61.
[25] S. Izumiya, M.d.C. Romero Fuster, M.A.S. Ruas, F. Tari, Differential Geometry from a Singularity Theory Viewpoint, World Scientific, 2015, http://dx.doi.org/10.1142/9108.
[26] A. Jain, A. Kapoor, Exact analytical solutions of the parameters of real solar cells using Lambert W-function, Sol. Energy Mater. Sol. Cells 81 (2) (2004) 269–277, http://dx.doi.org/10.1016/j.solmat.2003.11.018.
[27] K.L. Kennerud, Analysis of performance degradation in CdS solar cells, IEEE Trans. Aerosp. Electron. Syst. AES-5 (1969) 912–917, http://dx.doi.org/10.1109/TAES.1969.309966.
[28] K. Lappalainen, M. Piliougine, G. Spagnuolo, Experimental comparison between various fitting approaches based on RMSE minimization for photovoltaic module parametric identification, Energy Convers. Manage. 258 (2022) 115526, http://dx.doi.org/10.1016/j.enconman.2022.115526.
[29] A. Laudani, F. Mancilla-David, F. Riganti-Fulginei, A. Salvini, Reduced-form of the photovoltaic five-parameter model for efficient computation of parameters, Sol. Energy 97 (2013) 122–127, http://dx.doi.org/10.1016/j.solener.2013.07.031.
[30] A. Laudani, F. Riganti-Fulginei, A. Salvini, High performing extraction procedure for the one-diode model of a photovoltaic panel from experimental I–V curves by using reduced forms, Sol. Energy 103 (2014) 316–326, http://dx.doi.org/10.1016/j.solener.2014.02.014.
[31] A. Laudani, F. Riganti-Fulginei, A. Salvini, Identification of the one-diode model for photovoltaic modules from datasheet values, Sol. Energy 108 (2014) 432–446, http://dx.doi.org/10.1016/j.solener.2014.07.024.
[32] G.H. Light, Discussions: The existence of cusps on the evolute at points of maximum and minimum curvature on the base curve, Amer. Math. Monthly 26 (4) (1919) 151–154.
[33] V. Lo Brano, G. Ciulla, An efficient analytical approach for obtaining a five parameters model of photovoltaic modules using only reference data, Appl. Energy 111 (2013) 894–903, http://dx.doi.org/10.1016/j.apenergy.2013.06.046.
[34] B. Marion, M.G. Deceglie, T.J. Silverman, Analysis of measured photovoltaic module performance for Florida, Oregon, and Colorado locations, Sol. Energy 110 (2014) 736–744, http://dx.doi.org/10.1016/j.solener.2014.10.017.
[35] S. Mirjalili, A.H. Gandomi, S.Z. Mirjalili, S. Saremi, H. Faris, S.M. Mirjalili, Salp swarm algorithm: A bio-inspired optimizer for engineering design problems, Adv. Eng. Softw. 114 (2017) 163–191, http://dx.doi.org/10.1016/j.advengsoft.2017.07.002.
[36] D. Oliva, E. Cuevas, G. Pajares, Parameter identification of solar cells using artificial bee colony optimization, Energy 72 (2014) 93–102, http://dx.doi.org/10.1016/j.energy.2014.05.011.
[37] S.J. Patel, A.K. Panchal, V. Kheraj, Solar cell parameters extraction from a current-voltage characteristic using genetic algorithm, J. Nano Electron. Phys. 5 (1) (2013) 02008.
[38] J.C.H. Phang, D.S.H. Chan, J.R. Phillips, Accurate analytical method for the extraction of solar cell model parameters, Electron. Lett. 20 (1984) 406–408, http://dx.doi.org/10.1049/el:19840281.
[39] M. Piliougine, R.A. Guejia-Burbano, G. Petrone, F.J. Sánchez Pacheco, L. López, M. Sidrach-de-Cardona, Parameters extraction of single diode model for degraded photovoltaic modules, Renew. Energy 164 (2021) 674–686, http://dx.doi.org/10.1016/j.renene.2020.09.035.
[40] M. Schwartz, On the distance from a point to a curve, College Math. J. 25 (4) (1989) 317–319.
[41] H.L. Smith, A note on a distance formula of plane analytics, Math. News Lett. 3 (4) (1928) 19–21, http://dx.doi.org/10.1016/j.solener.2021.01.067.
[42] F.J. Toledo, J.M. Blanes, Geometric properties of the single-diode photovoltaic model and a new very simple method for parameters extraction, Renew. Energy 72 (2014) 125–133, http://dx.doi.org/10.1016/j.renene.2014.06.032.
[43] F.J. Toledo, J.M. Blanes, Analytical and quasi-explicit four arbitrary point method for extraction of solar cell single-diode model parameters, Renew. Energy 92 (2016) 346–356, http://dx.doi.org/10.1016/j.renene.2016.02.012.

[44] F.J. Toledo, J.M. Blanes, V. Galiano, Two-step linear least-squares method for photovoltaic single-diode model parameters extraction, IEEE Trans. Ind. Electron. 65 (8) (2018) 6301–6308, http://dx.doi.org/10.1109/TIE.2018.2793216.

[45] F.J. Toledo, J.M. Blanes, V. Galiano, A. Laudani, In-depth analysis of single-diode model parameters from manufacturer's datasheet, Renew. Energy 163 (2021) 1370–1384, http://dx.doi.org/10.1016/j.renene.2020.08.136.

[46] F.J. Toledo, J.M. Blanes, A. Garrigós, J.A. Martínez, Analytical resolution of the electrical four-parameters model of a photovoltaic module using small perturbation around the operating point, Renew. Energy 43 (2012) 83–89, http://dx.doi.org/10.1016/j.renene.2011.11.037.

[47] M.G. Villalva, J.R. Gazoli, E.R. Filho, Comprehensive approach to modeling and simulation of photovoltaic arrays, IEEE Trans. Power Electron. 24 (5) (2009) 1198–1208, http://dx.doi.org/10.1109/TPEL.2009.2013862.